EFFECT OF GEOMETRICAL IMPERFECTIONS ON THE RESPONSE OF DRY-JOINT MASONRY ARCHES TO SUPPORT SETTLEMENTS

CHIARA FERRERO[1,2]*, MICHELA ROSSI[1], PERE ROCA[2] AND CHIARA CALDERINI[1]

[1] Department of Civil, Chemical and Environmental Engineering
University of Genoa
Via Montallegro 1, 16154 Genoa, Italy
email: chiara.ferrero@edu.unige.it, michela.rossi@dicca.unige.it, chiara.calderini@unige.it
(* corresponding author)

[2] Department of Civil and Environmental Engineering
Technical University of Catalonia (UPC-BarcelonaTech)
Jordi Girona 1-3, 08034 Barcelona, Spain
e-mail: pere.roca.fabregat@upc.edu

Keywords: Masonry arches, Experimental tests, FE micro-modelling, Support displacements, Collapse mechanisms, Geometrical imperfections.

Abstract. *This paper aims to investigate the effects of geometrical imperfections on the response of a scaled dry-joint arch to the vertical displacement of one support. The arch behaviour was analysed in the large displacement regime using both physical and numerical modelling. The experimental tests were performed on 1:10 small-scale models made of bi-component composite blocks with dry joints. In order to evaluate the geometrical accuracy of the blocks, two different sets of voussoirs were produced. The numerical simulations were carried out using a finite element (FE) micro-modelling approach, where the arch was modelled as an assembly of very stiff voussoirs connected by nonlinear interfaces. Particular attention was paid to the interface stiffness, which was set so as to tune the numerical model with the experimental evidence. Experimental and numerical results were then compared in terms of collapse mechanism, hinge configuration and ultimate displacement capacity. The imperfections of the physical models were found to significantly affect the arch response.*

1 INTRODUCTION

The safety assessment of masonry arches is a crucial issue for the conservation of cultural heritage, as arches have been often used as structural elements in historic masonry constructions. Masonry arches are sensitive to any change in the external environment and thus crack when the abutments move. Support movements can be produced by a wide range of different causes, including differential settlements, subsidence, landslides, soil heterogeneity, instability of the supporting walls/pillars, construction defects and many others. Although small

movements do not represent a threat to stability since they can be easily accommodated by arches through the opening of some cracks (idealized as hinges [1]), large movements involving progressive changes in the geometry may lead to serious damage and collapse.

Over the years, considerable research effort has been devoted to finding new methods and computational tools to investigate the response of masonry arches to large support displacements. Several analytical methodologies were developed to evaluate the collapse mechanisms and ultimate displacement capacity of masonry arches with different geometries subjected to spreading supports (e.g. [2-4]) or generic support displacements (e.g. [5-7]). In the framework of numerical methods, different computational approaches were proposed to investigate the response of arches and, more in general, masonry structures to support displacements, such as finite element (FE) modelling (e.g. [8-10]), discrete element (DE) modelling (e.g. [11]) and rigid block modelling (e.g. [12,13]), among others. Nevertheless, both analytical and numerical methods require to be validated against experimental tests to prove their capability of accurately simulate the collapse of masonry structures. For this reason, the analytical and numerical predictions were often validated by comparison with the results from small-scale model testing (for arches on moving supports, the reader is referred to [2,5-10]). Compared to full-scale models, small-scale models offer several advantages, such as short set-up times, reduced cost, and possibility to repeat the experiments several times. Furthermore, as first demonstrated by Heyman [1], they are effective to predict the collapse of masonry structures, which depends mainly on geometry rather than material strength and thus can be studied independently on scale. This also explains why physical scale-models have been widely used to investigate the stability of masonry arches and vaults not only under support displacements, but also under seismic actions (e.g. [14-18]) or point loads (e.g. [18,19]).

In the case of arches and vaults on moving support, the comparison between analytical and numerical predictions on one side and experimental evidence on the other side showed that both analytical and numerical models are generally able to capture accurately the collapse mechanisms of the physical models. However, they tend to overestimate the displacement capacity obtained experimentally (see [2,5,20,21]). As described in [5,20,21], this behaviour can be attributed to the imperfections and assembly inaccuracies that characterize the physical models compared to the "perfect" numerical ones. More in detail, the imperfections in the dimension of the individual blocks as well as the manual assembly of the physical models, which cannot be perfect, can lead to an inaccurate interlocking between the blocks. Furthermore, the edges of the blocks can become rounded if tests are repeated several times. The combination of these factors result in a reduction of the effective thickness of the physical models, causing collapse to occur for smaller ultimate displacements than the ones predicted by analytical or numerical simulations. A similar effect was also observed when testing small-scale arches under seismic actions. In this case, in order to take into account the imperfections of the physical models and tune the numerical results with the experimental evidence, several authors (e.g. [15-17,22]) proposed to consider a reduced thickness in the numerical models.

In this work, the effect of geometrical imperfections on the response of scaled dry-joint masonry arches to the settlement of one support was investigated through experimental tests and numerical simulations. The experimental tests were performed on 1:10 small-scale models built as dry-joint assemblages of bi-component composite voussoirs. Two sets of voussoirs with

different geometrical accuracies were produced by using different manufacturing techniques. The numerical simulations of the experimental tests were carried out by adopting a FE micro-modelling approach, according to which the arch was modelled as an assembly of very stiff voussoirs connected by no-tension friction interfaces. Differently from what proposed in the literature for small-scale arches subjected to seismic actions, the numerical results were here tuned with the experimental evidence by properly setting the stiffness of the interface elements. This approach was already adopted by the authors in [10] for the simulation of the experimental tests performed using one of the two sets of voussoirs.

The aims of this work were (i) to evaluate to what extent the imperfections of the physical models can affect the arch behaviour in terms of collapse mechanism, hinge position and displacement capacity, and (ii) to assess the capability of the proposed FE micro-modelling approach to simulate the experimental response.

2 EXPERIMENTAL TESTS

The experimental tests were performed on a 1:10 small-scale model of a segmental dry-joint arch supported by two piers (Figure 1, Figure 2). The arch geometry was determined taking as a reference the cross-section of the barrel vaults that are generally used as ceiling in the main nave of historic masonry churches. More specifically, a two-course brick barrel vault with a radial thickness of 0.24 m and a net span of 6 m was considered. It is worth noting that, when this type of vaults is used as a ceiling and not as a load-bearing floor, it does not typically include any backfill. Instead, it is structurally merged with the supporting walls at the abutments. For this reason, the springings of the physical model were considered at about 27° from the horizontal plane.
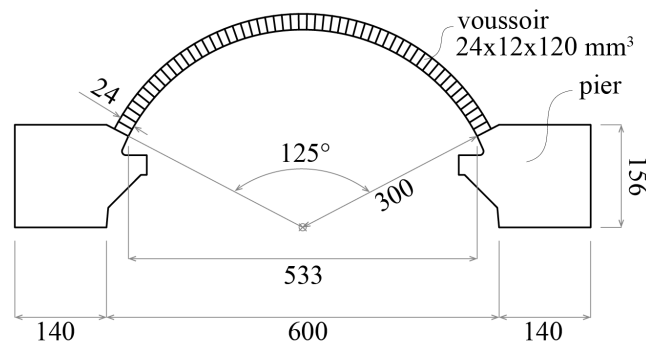
Figure 1: Geometry of the arch mock-up (in mm).

Figure 1 shows the geometry of the mock-up. The arch has an angle of embrace of 125°, an internal radius of 300 mm, a net span of 533 mm, a radial thickness of 24 mm and a depth of 120 mm. It is composed of 55 voussoirs with a height of 24 mm and a width of about 12 mm. Each voussoir represents the scaled dimensions of two adjacent bricks of standard size (60x120x240 mm^3) positioned with their longest side along the radial plane. The voussoirs are slightly trapezoidal in shape in order to compensate for the lack of mortar between them. The piers are shaped in such a way that they can sustain the plywood scaffolding needed to build

the arch (Figure 2a).

a)   b)
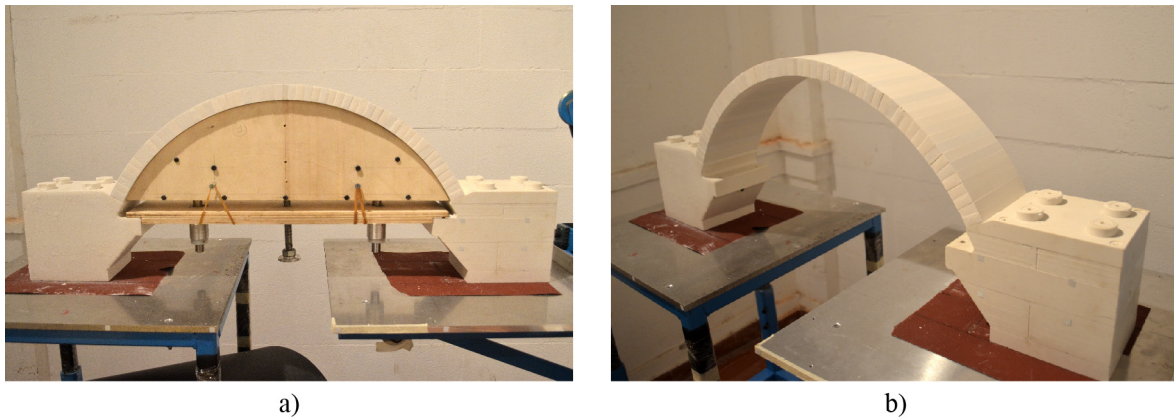
Figure 2: Physical model: a) plywood scaffolding, b) view after the removal of the scaffolding.

All the blocks (voussoirs and piers) are made of a bi-component composite material, obtained by mixing a mineral powder with an acrylic polymer in aqueous solution. The mixture was poured, let it harden and then removed from special silicone moulds (Figure 3), which were created using aluminium matrices shaped as the blocks. The density of the blocks was measured to be 1.64 g/cm^3 and the friction angle 41.2°. The Young's modulus, determined by compressive tests (see [10]), was equal to 941 MPa.

Since this manufacturing technique is innovative in the framework of small-scale model testing, the dimensional accuracy of the blocks was evaluated by producing two different sets of voussoirs (Figure 3).


a)   b)
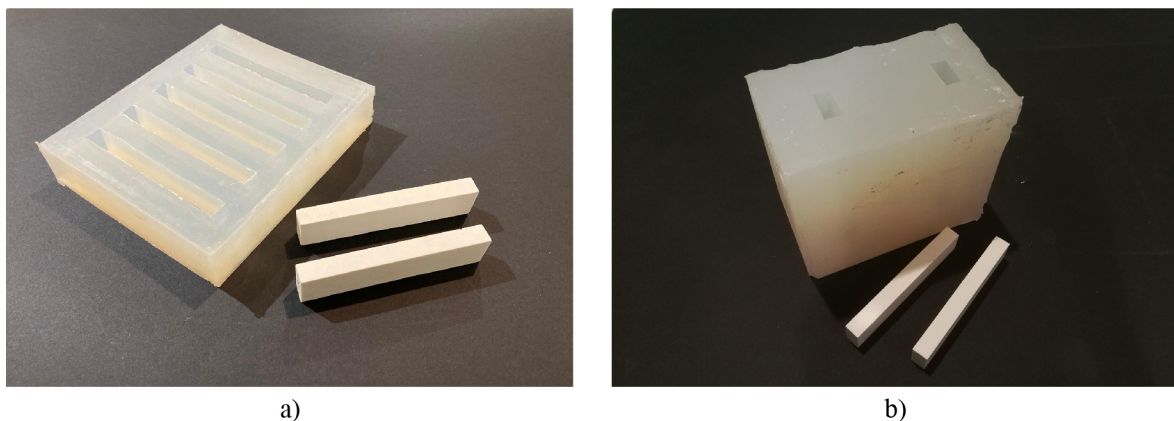
Figure 3: Silicone moulds used to produce the voussoirs: a) 1st set, b) 2nd set.

For the 1st set of voussoir, the aluminium matrices were manufactured using a manual milling machine; the mould was made of a deformable silicone and was created by positioning the aluminium matrices with their longest side horizontal (Figure 3a); the mixture was not vibrated; no admixtures were added to the bi-component composite material. For the 2nd set of voussoirs,

the aluminium matrices were produced through a CNC machine (precision ±0.05mm); the mould was made of a stiffer silicone and was manufactured placing vertically the longest side of the aluminium matrices (Figure 3b); the mould was vibrated mechanically in order to eliminate the air bubbles from the freshly poured mixture; the mixture was fluidified by adding a plasticizer (1% of the total weight).

The two sets of voussoirs are significantly different. The voussoirs of the 1st set (Figure 4a) have more imperfections and less sharp corners compared to the voussoirs of the 2nd set (Figure 4b). Furthermore, when they are placed side by side, their lateral faces are not perfectly coplanar (Figure 4a). The use of a manual milling machine to produce the voussoirs of the 1st set did not allow an accurate reproduction of the trapezoidal shape of the individual blocks. This resulted in a not perfect interlocking between voussoirs, causing gaps and hinges to occur (Figure 4c). Conversely, when a CNC machine was used to manufacture the blocks of the 2nd set, the assembly was very accurate and no gaps between adjacent voussoirs were observed (Figure 4d).

a)

b)

c)

d)
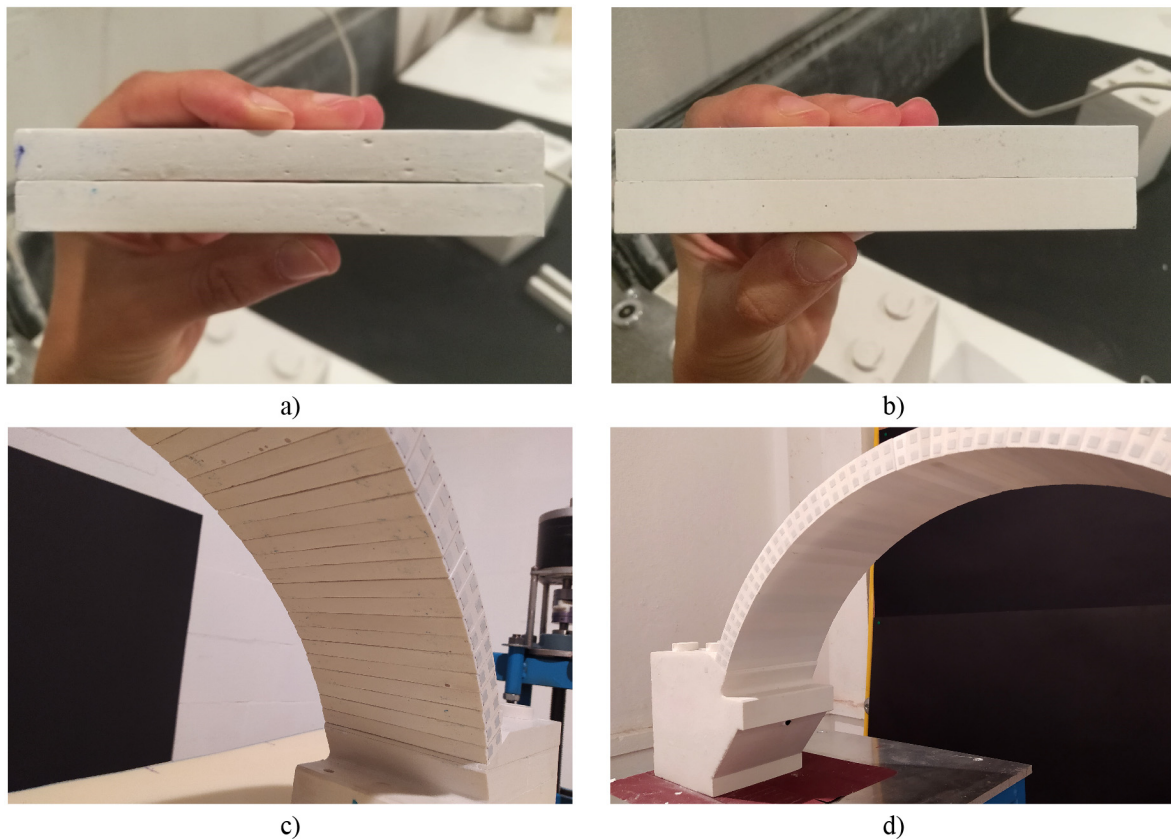
Figure 4: Different sets of voussoirs produced: a-c) 1st set, b-d) 2nd set.

Figure 5 depicts the initial geometry of the physical models created using either set of voussoirs. The shape of the two models is slightly different since the keystone of the arch built with the 1st set of voussoirs descended by few millimetres as soon as the scaffolding was removed (Figure 5a), while no significant movement was noticed for the arch built using the

2nd set of voussoirs (Figure 5b). It is worth noting that the downward displacement of the keystone observed for 1st set of voussoirs produced a slightly change in the geometry of the free-standing arch with respect to the "perfect" one shown in Figure 1.
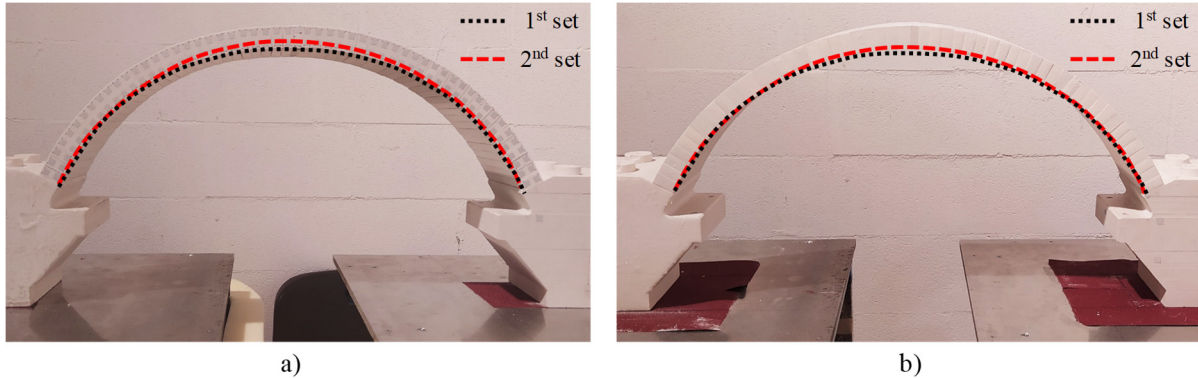
Figure 5: Initial geometry of the arch after the removal of the scaffolding: a) 1st set of voussoirs, b) 2nd set of voussoirs.

The arch was tested under an increasing downward quasi-static vertical displacement δ applied at the right support through an external stepper motor linear actuator controlled via software (Figure 6a). Two high-resolution, high-frame rate (60 Hz) cameras were used to record the development of the damage up to collapse (Figure 6b).
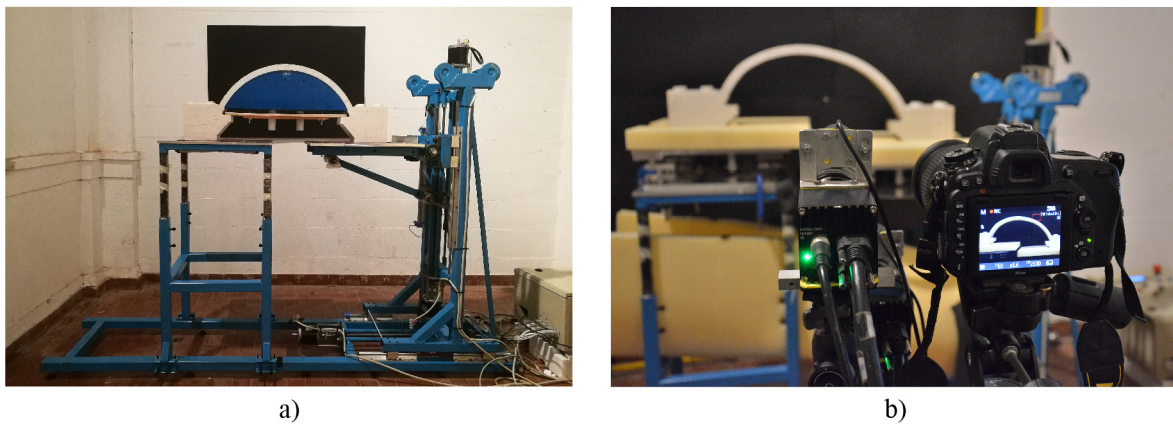
Figure 6: a) Testing machine, b) high-resolution, high-frame rate cameras.
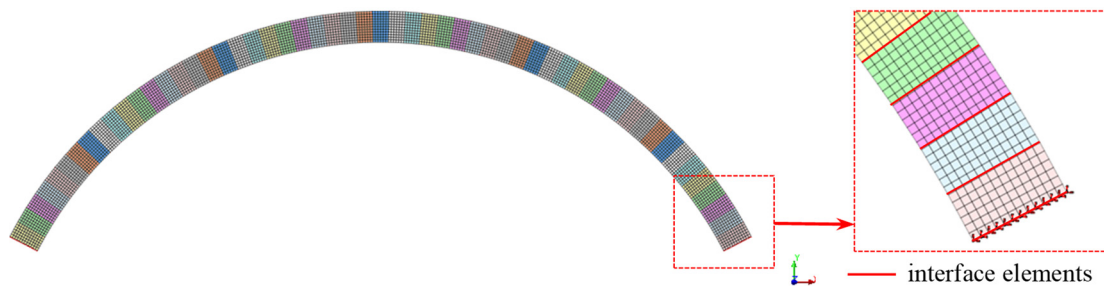
3 FINITE ELEMENT MICRO-MODELLING

The numerical simulations of the experimental tests were performed through the FEM software DIANA [23]. A two-dimensional FE model of the arch was created in Midas FX+ Version 3.3.0 (Customized Pre/Post-processor for DIANA software [24]) adopting a micro-modelling approach, where each voussoir was modelled as a distinct (very stiff) block and dry joints were represented as no-tension frictional interfaces placed in between the voussoirs.

Further interface elements were placed at the springing of the arch to allow for hinge opening at the supports. The piers were not included in the FE model, as they only provided support to the arch.

Four-node quadrilateral isoparametric plane stress elements (Q8MEM) were used to model the voussoirs, while 2D four-node line interface elements (L8IF) were employed for the interfaces. A mesh size of 2 mm (i.e. 12 FEs elements along the arch radial thickness) was adopted based on a sensitivity analysis on the ultimate vertical displacement δ_u obtained at collapse. For further details about the mesh sensitivity analysis, the reader is referred to [10].

The mesh of FE micro-model of the arch, composed of 5031 nodes and 4632 elements, is presented in Figure 7. Note that the outer edges of the interface elements placed at the supports were pinned to provide boundary conditions.


Figure 7: FE micro-model of the arch.

The voussoirs were modelled as linear elastic elements with infinite compressive strength. Young's modulus and mass density were set equal to 941 MPa and 1.64 gr/cm^3, respectively, in accordance with the values measured experimentally (see section 2). A Poisson's ratio of 0.2 was assumed. For the interface elements, a Coulomb friction model was used. Cohesion and dilatancy angle were set equal to zero, while a friction angle of 41.2° was adopted, as measured for the voussoirs of the physical model. In order to simulate hinge opening, the friction criterion was extended with a gap criterion [23] with zero tensile strength. For further details about the Coulomb friction model, the reader is referred to [23].

The stiffness of the interface elements was evaluated through a sensitivity analysis (Figure 8), where the collapse displacement δ_u was determined for different values of k_n in the range 0.1÷100 N/mm^3 (this latter was defined according to the values proposed in [16]). The interface tangential stiffness k_s was set equal to 0.5k_n for any considered value of k_n. This choice was made only to optimize numerical convergence, since the ratio between the two stiffnesses did not influence the arch structural response. As described by the authors in [10], very large stiffness values simulate rigid contact surfaces, allowing to treat the arch as a rigid-no tension structure, but they lead to significantly overestimate the displacement capacity obtained from experimental methods. Conversely, reduced stiffness values enable to consider the imperfections (and resulting deformability) that characterize the contact surfaces of the physical models. With the aim of simulating the experimental tests, the interface normal stiffness was chosen so that the numerical collapse displacement matched closely the experimental result for

each of the two sets of voussoirs considered. Consequently, k_n was set equal to 0.25 N/mm^3 and 5.2 N/mm^3 for the 1st and 2nd sets of voussoirs, respectively.
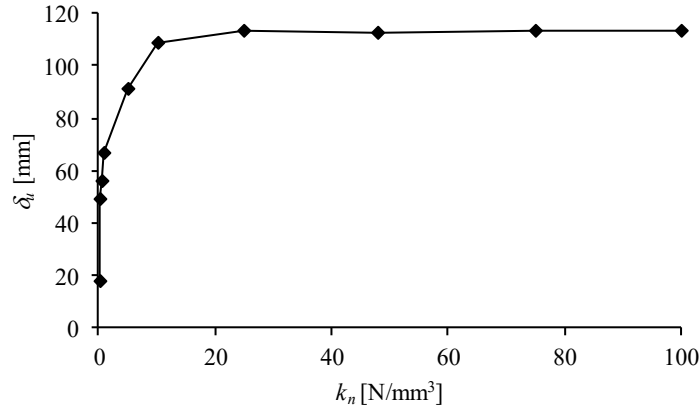
Figure 8: Collapse displacement δ_u vs. interface normal stiffness k_n.

The response of the arch to large support displacements was evaluated through non-linear static analyses. After the application of the self-weight, the imposed vertical displacement δ was increased monotonically until collapse was reached. A regular Newton-Raphson iteration method combined with a line search algorithm was employed. An energy-based convergence criterion with a tolerance value of 0.001 was assumed. Geometrical non-linearities were taken into account by adopting the Total Lagrange formulation available in DIANA [23].

4 EXPERIMENTAL VS. NUMERICAL RESULTS

This section presents and compares the experimental and numerical results obtained from both sets of voussoirs in terms of collapse mechanisms (Figure 9) as well as hinge position and ultimate displacement at collapse δ_u (Table 1). In Table 1, the interfaces where hinges appear are numbered from left to right, being interface no. 1 the interface at the left support.

The collapse mechanisms obtained from the experimental test and relevant numerical simulation for the 1st of voussoirs are illustrated in Figure 9a-c. In the experimental test (Figure 9a), three hinges, A, B and C, initially occurred in the sequence I-E-E (from left to right, where E = extrados; I = intrados). Hinge A was located at the haunches between 11th and 12th voussoirs (interface no. 12), hinge B appeared close to midspan between 31st and 32nd voussoirs (interface no. 32), and hinge C opened at the right support (interface no. 56). Hinges B and C remained in their initial position and did not move as the imposed vertical displacement increased. Conversely, hinge A moved towards the crown by one voussoir just before collapse. The arch collapsed by an asymmetrical four-hinge mechanism when a fourth hinge (D) occurred at the left support at the extrados for a vertical displacement of 48.9 mm (Figure 9a).

Figure 9c illustrates the collapse mechanism predicted by FE analyses when adopting a value of k_n equal to 0.25 N/mm^3. For the latter, the numerical collapse displacement δ_u (48.8 mm) matched very closely the experimental one. Collapse occurred again by an asymmetrical four-hinge mechanism with hinges located according to the sequence E-I-E-E. The predicted final

8

hinge position agreed well with the experimental results since hinges B, C and D appeared at the same location of the physical model, and hinge A was shifted by one voussoir only. Differently, hinge A did not move with increasing support displacements. Despite the good agreement in terms of displacement capacity and hinge position, the FE analysis did not perfectly capture the actual behaviour of the physical model, since hinges A and B, which concentrated in one single interface in the test, appeared to be distributed over adjacent interfaces in the numerical simulation. Nevertheless, this discrepancy could be attributed to the not perfect geometry of the physical model, which was slightly different from the numerical one since the keystone descended by few millimetres after the scaffolding was removed (as already shown in Figure 5).

Figure 9b and Figure 9d show the collapse mechanisms obtained for the 2nd set of voussoirs from the experimental test and numerical simulation, respectively. In the test, the three initial hinges A, B and C appeared in the sequence I-E-E and did not move as the support displacements increased. The position of hinges B and C was very similar to that obtained for the 1st set, since hinge C occurred again at the left support and the location of hinge B differed by only one block, opening between 30th and 31st voussoirs (interface no. 31). However, a significant difference was found in the final position of hinge A, which appeared four blocks closer to the left support (interface no. 9) in the 2nd set compared to the 1st set. The failure mode was the same as that obtained for the 1st set of voussoirs, since collapse occurred when the fourth hinge D appeared at the left support. Nevertheless, the collapse displacement δ_u was significantly larger, being equal to 91.5 mm. As can be observed from Figure 9d, the numerical results obtained for k_n equal to 5.2 N/mm^3 (δ_u = 91.8 mm) were in very good agreement with the experimental results in terms of both collapse mechanisms and hinge position. As for the latter, the predicted position of hinges A, C and D was in full accordance with the experimental tests, while hinge B was shifted by only one voussoir. As already observed in the test, also in the numerical simulation all hinges remained in their initial position and did not move with increasing support displacements.

Table 1: Comparison of numerical and experimental results in terms of hinge position (indicated with the interface where hinges appear, numbered from left to right) and collapse displacement δ_u.

	1st set of voussoirs		2nd set of voussoirs	
	Experimental	Numerical	Experimental	Numerical
Position of hinge A at collapse	13	11-12	9	9
Position of hinge B at collapse	32	29-30-31-32	31	30
Position of hinge C at collapse	56	56	56	56
Collapse displacement δ_u [mm]	48.9	48.8	91.5	91.8
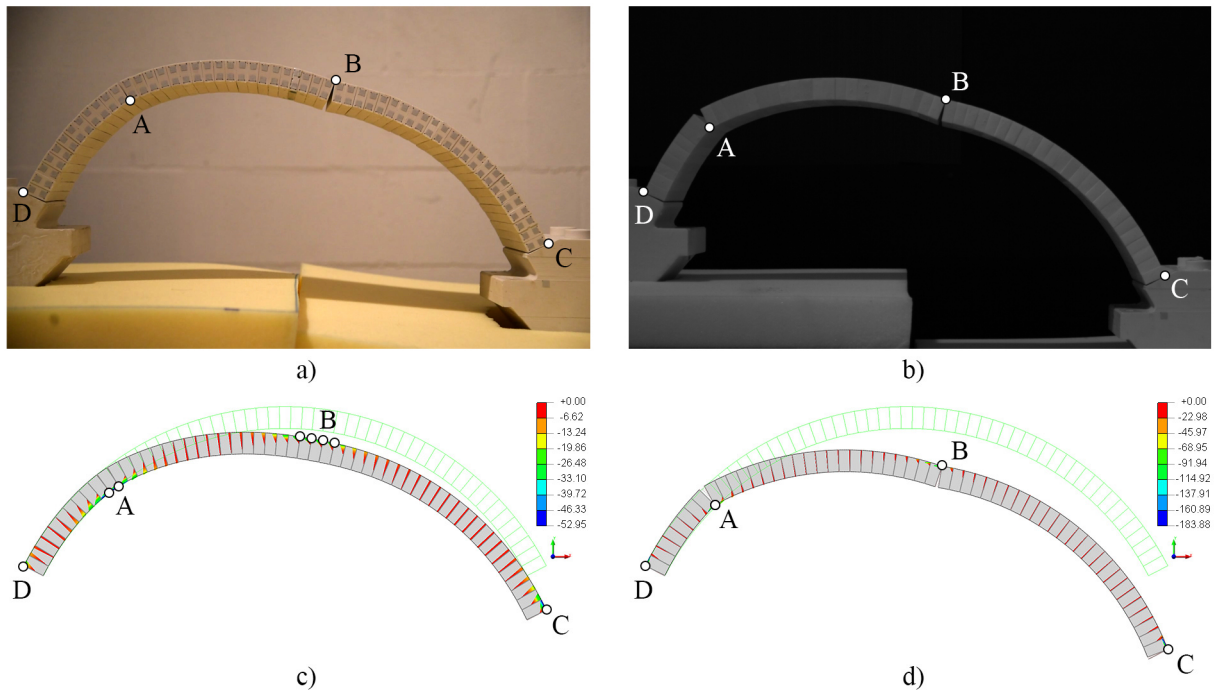
Figure 9: Collapse mechanism obtained using the 1st set (left) and 2nd set (right) of voussoirs: a-b) experimental tests, c-d) numerical simulations.

5 CONCLUSIONS

In this paper, the response of a segmental dry-joint masonry arch to the vertical displacement of one support was investigated using both physical and numerical modelling. With the aim of evaluating the effect of geometrical imperfections on the arch response, two different sets of voussoirs with different geometrical accuracies were employed to build the small-scale models. The experimental tests were then simulated through FE micro-modelling. The stiffness of the interface elements used to model the dry joints was calibrated so that the ultimate displacement capacity obtained numerically matched closely the experimental one.

The results of the experimental tests proved that the imperfections and assembly inaccuracies of the physical models significantly affect the arch response, especially in terms of displacement capacity. Indeed, although the same collapse mechanism occurred for either set of voussoirs, the collapse displacement obtained using the 1st set, which was characterized by more imperfections, was significantly lower than that obtained with the 2nd set.

For both sets of voussoirs, the numerical predictions were in good agreement with the experimental results in terms of collapse mechanism, hinge position and displacement capacity. This demonstrated that calibrating the interface stiffness based on the experimental evidence is an effective strategy to accurately capture the experimental response of dry-joint masonry arches to large support displacements. The difference in the hinge distribution obtained when simulating the test performed using the 1st set of voussoirs can be explained considering that the geometry of the physical model was slightly different from the perfect numerical one.

In conclusion, this work provides a contribution for a better understanding of the effect of geometrical imperfections on the response of scaled dry-joint masonry arches. Future works will include the application of different configurations of support displacements as well as the measurement of the reactions at the arch supports in the experimental tests. This will allow to evaluate the effect of geometrical imperfections on the arch response in terms of support reaction-displacement curves.

REFERENCES

[1] Heyman, J. *The stone skeleton. Structural engineering of masonry architecture*. Cambridge University Press, Cambridge (1995).

[2] Ochsendorf, J. A. The masonry arch on spreading supports. *Struct. Eng.* (2006) **84**(2):29-35.

[3] Coccia, S., Di Carlo, F. and Rinaldi, Z. Collapse displacements for a mechanism of spreading-induced supports in a masonry arch. *Int. J. Adv. Struct. Eng.* (2015) **7**(3):307-320.

[4] Di Carlo, F. and Coccia, S. Collapse state of elliptical masonry arches after finite displacements of the supports. *Eng. Fail. Anal.* (2020) **114**.

[5] Galassi, S., Misseri, G., Rovero, L. and Tempesta, G. Failure modes prediction of masonry voussoir arches on moving supports. *Eng. Struct.* (2018) **173**:706-717.

[6] Zampieri, P., Simoncello, N. and Pellegrino, C. Structural behaviour of masonry arch with no-horizontal springing settlement. *Frat. ed Integrità Strutt.* (2018) **12**(43):182-190.

[7] Smars, P. Kinematic Stability of Masonry Arches. *Adv. Mater. Res.* (2010) **133-134**:429-434.

[8] Alforno, M., Monaco, A., Venuti, F. and Calderini, C. Validation of Simplified Micro-models for the Static Analysis of Masonry Arches and Vaults, *Int. J. Archit. Herit.* (2020).

[9] Masciotta, M-G., Pellegrini, D., Girardi, M., Padovani, C., Barontini, A, Lourenço, PB, Brigante, D. and Fabbrocino, G. Dynamic characterization of progressively damaged segmental masonry arches with one settled support: experimental and numerical. *Frat. ed Integrità Strutt. (*2020) **51**:423-441.

[10] Ferrero, C., Rossi, M., Roca, P. and Calderini, C. Experimental and numerical analysis of a scaled dry-joint arch on moving supports. *Int. J. Mason. Res. Innov.* (2020).

[11] McInerney, J. and DeJong, M. J. Discrete Element Modeling of Groin Vault Displacement Capacity. *Int. J. Archit. Herit.* (2015) **9**(8):1037–1049.

[12] Gilbert, M. and Melbourne, C. Rigid-block analysis of masonry structures. *Struct. Eng.* (1994) **72**(21).

[13] Portioli, F. and Cascini, L. Large displacement analysis of dry-jointed masonry structures subjected to settlements using rigid block modelling. *Eng. Struct.* (2017) **148**:485-496.

[14] Calderini, C., Lagomarsino, S., Rossi, M., De Canio, G., Mongelli, M.L. and Roselli, I. Shaking table tests of an arch-pillars system and design of strengthening by the use of tie-rods. *Bull. Earthq. Eng* (2015) **13**(1):279–297.

[15] DeJong, M., De Lorenzis L., Adams, S. and Ochsendorf J.A. Rocking stability of masonry arches in seismic regions. Earthq. Spectra (2008) **2**:847–865.

[16] Gaetani, A., Lourenço P. B., Monti, G. and Moroni, M. Shaking table tests and numerical analyses on a scaled dry-joint arch undergoing windowed sine pulses. *Bull. Earthq. Eng.* (2017) **15**:4939-4961.

[17] Misseri, G., DeJong, M.J. and Rovero, L. Experimental and numerical investigation of the collapse of pointed masonry arches under quasi-static horizontal loading. *Eng. Struct.* (2018) **173**:180-190.

[18] Shapiro E.E. *Collapse mechanism of small-scale unreinforced masonry vaults*. M.S. thesis in Building Technology, Massachusetts Institute of Technology (2012).

[19] Pippard A.J.S. and Ashby, R. An experimental study of the voussoir arch. *J. Inst. Civ. Eng Journal of the Institution of Civil Engineers* (1939) **10**(3):383-404.

[20] Van Mele, T., McInerney, J., DeJong, M. and Block P. Physical and Computational Discrete Modelling of Masonry Vault Collapse,' In: *Proceedings of 8th International Conference on Structural Analysis of Historical Constructions,* (2012), pp. 2552–2560.

[21] Quinonez, A., Zessin, J., Nutzel, A. and Ochsendorf J.A. Small-Scale Models for Testing Masonry Structures. *Adv. Mater. Res.* (2010) **133–134**:497–502.

[22] Albuerne, A, Williams, M and Lawson V. Prediction of the failure mechanism of arches under base motion using DEM based on the NSCD method. Wiadomości Konserw (2013) **34**:41–47.

[23] TNO DIANA BV. DIANA Finite Element Analysis User's Manual Release 9.6, Delft, The Netherlands (2014).

[24] Midas FX+ for DIANA, Customized Pre/Post-processor for DIANA (2013).